INTERNATIONAL UNION OF
PURE AND APPLIED CHEMISTRY

MACROMOLECULAR DIVISION

A Collaborative Investigation into
The Rheology of Some Polystyrene
and Polyethylene Melts

A COLLABORATIVE INVESTIGATION INTO THE RHEOLOGY OF SOME POLYSTYRENE AND POLYETHYLENE MELTS

A Report of the IUPAC Working Party on The Relationship of Performance Characteristics to Basic Parameters of Polymers

Prepared for publication by

J. L. S. WALES
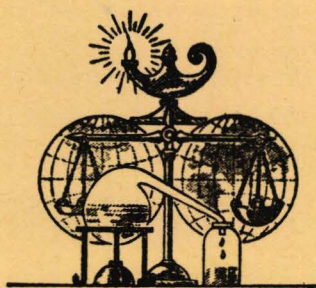
Centraal Laboratorium TNO,
Delft, Holland

MACROMOLECULAR DIVISION

A COLLABORATIVE INVESTIGATION INTO THE RHEOLOGY OF SOME POLYSTYRENE AND POLYETHYLENE MELTS*

SUMMARY

This report is a compilation of the work carried out by different laboratories participating in the IUPAC Working Party on 'The Relationship of Performance Characteristics to Basic Parameters of Polymers'. The object was to study the relationship between processing and fundamental molecular structure. As a step in this direction participating laboratories have made various rheological measurements on six molten polymers: two polystyrenes, two low density polyethylenes and two high density polyethylenes. Each pair consisted of one material with a narrow molecular weight distribution and one with a broader molecular weight distribution. Measurements of viscosity in steady flow, dynamic viscosity, flow birefringence and stress-relaxation have been carried out. The participants are in general agreement about the relative shapes of the flow curves for steady shear flow and their temperature dependency although full agreement about the absolute values of the viscosities has not been obtained at all shear rates. A definite correspondence between the dynamic viscosity $|\eta^*(\omega)|$ and the steady flow viscosity $\eta(q)$ is found. Good agreement is found between spectra of relaxation times calculated from $G'(\omega)$, $G''(\omega)$ and from stress-relaxation after steady shear flow. Flow birefringence measurements demonstrated that increasing polydispersity implies increasing elasticity.

1. INTRODUCTION

Viscosity and elasticity are considered to be important parameters for the processing of polymeric materials. The quantitative measurement of these parameters in a much simpler flow system than occurs in any processing machine is felt useful for qualitative characterization of material for the more complicated flow situation that will invariably occur in industrial practice. For instance if two materials have similar viscosities but differing elastic properties in flow, one might expect the finished product made from them to have differing amounts of mechanical anisotropy owing to the differing orientation arising during processing.

Simple shear deformation and flow is almost invariably chosen to characterize visco-elastic liquids as this is experimentally the most readily amenable. Nevertheless, even with this single method the number of

---

available devices which can be used to characterize materials is rather large and it is therefore too much for a single laboratory to carry out tests with all possible devices.

For this reason a joint attack on the problem of material characterization is often desirable. To this end a group of laboratories within the 'Working Party on the Relationship of Performance Characteristics to Basic Parameters of Polymers' of IUPAC Macromolecular Division have pooled their efforts into the measurement of six polymers: two polystyrenes, two low density polyethylenes and two high density polyethylenes. Each pair of polymers consisted of one material with a relatively broad molecular weight distribution and one material with a relatively narrow molecular weight distribution.

The laboratories which participated in the experimental work are listed below:

I. Monsanto	Newport	Great Britain
II. Péchiney-Saint-Gobain	Antony	France
III. Solvay	Brussels	Belgium
IV. TNO	Delft	Netherlands

For convenience, henceforth the above laboratories will be referred to by the Roman numerals given for these laboratories.

The materials were rheologically characterized by the following methods.

Steady simple shear flow
   A. I and III carried out capillary viscometry measurements under conditions of constant output and constant pressure, respectively.
   B. IV carried out slit viscometry measurements under conditions of constant output.
   C. II carried out cone-and-plate viscometry measurements.
   D. IV carried out flow birefringence measurements with a cone-and-plate apparatus.

Oscillatory simple shear deformation (dynamic measurements)
   E. IV carried out measurements with an apparatus of concentric cylinder geometry.

Stress relaxation after steady simple shear flow
   F. II carried out measurements with a cone-and-plate apparatus.

2. SPECIFICATION OF THE APPARATUSES

I The now commercially available instrument known as the Instron Rheometer, similar to the one originally developed by Merz and Colwell[1]. For the polystyrene work a single capillary of 60 L/R; $R = 0.026$ cm and 30° entrance angle was used. For polyethylene most of the work was carried out with a single capillary of 120 L/R; $R = 0.08026$ cm and 90° entrance angle, but some results were obtained with a 120 L/R; $R = 0.03993$ cm capillary and 90° entrance angle.

II The Kepes cone-and-plate viscometer used for both steady flow viscosity determination and for stress-relaxation. Radius of cone 2·615 cm; angle between cone and plate 0·039 radians. The stress-relaxation after steady shear flow was followed by a Tektronix oscilloscope.

III Gas driven capillary rheometer, manufactured by Canadian Industrial Limited. A single capillary of 28·4 L/R; $R = 0.0532$ cm and 90° entrance angle was used.

IV Slit viscometer—own manufacture, piston driven viscometer similar to that described by Wales et al[2]. Channel length 11 cm, slit 1 cm × 0·05 cm and entrance angle 180°.

Cone-and-plate birefringence apparatus—own manufacture, fully described in literature[3]. Radius of cone 2·5 cm, angle between cone and plate 0·02 radians.

Dynamic viscometer—own manufacture, concentric cylinder device, radius of inner cylinder = 0·5 cm, radius of outer cylinder 0·9 cm. Fully described in literature[4].

3. THE MATERIALS

Polystyrenes. Supplied by Dow Chemical Company and designated S III and B 8. Their characteristics were also reported as follows:

	M_n	M_w	M_w/M_n
S 111	2.14×10^5	2.24×10^5	1·04
B 8	1.13×10^5	2.79×10^5	2·47

Low density polyethylenes. Supplied by Monsanto Chemical Company with the designations Sample A: LP 174 D and Sample B: MPE 76 (Blend 9801). These will henceforth be referred to as LDPE-A and LDPE-B, respectively. Dr. Drott of Monsanto kindly evaluated molecular weight distributions from G.P.C. measurements using trichlorobenzene as solvent and neglecting the effect of 'peak broadening'. Dr. Panaris of N.P.A. also kindly furnished light scattering and G.P.C. data.

Table 1 gives molecular weight data as well as the source.

Table 1. Molecular weight data and the source of low density polyethylenes

Molecular weight	Method	Source	LDPE-A	LDPE-B
M_n	Vapour pressure	I	1.5×10^4	1.28×10^4
	G.P.C.	Drott	1·5	1·47
	Osmometry	I	2·22	2·31
M_w	Light scattering	Panaris	12·5–13·3	24·7–27·5
	G.P.C.	Drott	7·95	21·3
M_z	G.P.C.	Drott	31·6	242

Laboratory II also estimated the following branching characteristics from infrared measurements:

LDPE-A: $CH_3/100\ CH_2 = 1.2$
LDPE-B: $CH_3/100\ CH_2 = 1.5$

High density polyethylenes. Designations HDPE-NMWD and HDPE-BMWD, supplied by Dow Chemical Company along with viscosity average molecular weights.

Table 2. Molecular weight data and the source of high density polyethylenes

Molecular weight	Method	Source	HDPE-NMWD	HDPE-BMWD
M_n	G.P.C.	Panaris	7.5×10^3	11.6×10^3
	G.P.C.	Drott	9.93	17.1
M_v	Viscosity	Dow	41.7	91.5
M_w	G.P.C.	Panaris	60.0	120.7
	G.P.C.	Drott	66.4	168
	Light scattering	Panaris	50	150
M_z	G.P.C.	Panaris	567	866.6
	G.P.C.	Drott	337	1500

For all the materials Gel Permeation Chromatograms (G.P.C.) have been made and will be available on request.

4. THE MEASUREMENTS

A. Capillary viscometry

The measured quantities are volume output per second (Q) and the pressure (P) before the entrance to the capillary. The following equations relate these quantities to the shear rate (q) and shear stress (τ) at the capillary wall.

$$q = \frac{D_c}{4}\left[3 + \frac{d \ln D_c}{d \ln \tau}\right] \tag{1}$$

$$\tau = \frac{P}{2}\left[\frac{L}{R} + n\right]^{-1} \tag{2}$$

$$D_c = \frac{4Q}{\pi R^3} \tag{3}$$

where R = radius of capillary
 L = length of capillary
 n = entrance correction—supposed to be independent of (R/L).

In the event that n is not measured the quantity $PR/2L$ is referred to as the apparent shear stress (τ_a) at the wall. D_c is called the apparent shear rate at the wall since for Newtonian liquids it is equal to q.

Laboratory I, using a ram viscometer, obtained Q from the ram speed and the dimensions of the rheometer. Laboratory III, using a gas pressure viscometer, obtained Q by weighing the output and converting to volume output with their experimentally found relation for the polyethylenes.

$$\rho = 0.7252 + (T_c^0 - 190) \times 6.06 \times 10^{-4}$$

B. Slit viscometry

Measured are the volume output per second (Q), obtained from the ram speed and the dimensions of the reservoir, and the pressure distribution along the slit channel $P(l)$. These are related to the shear rate at the wall q and the shear stress at the wall τ by the following:

$$q = \frac{D_s}{3} \left[2 + \frac{d \ln D_s}{d \ln \tau} \right] \tag{4}$$

$$D_s = \frac{6Q}{ab^2} \tag{5}$$

$$\tau = \lim_{l \to 0} \frac{P(l)}{2l} b \tag{6}$$

where a = long side of rectangular cross-section of channel
$\quad\;\; b$ = short side of rectangular cross-section of channel
$\quad\;\; l$ = distance from exit

D_s is called the apparent shear rate at the wall.

C. Cone-and-plate viscometry

The measured quantities are an applied angular velocity and the subsequent steady couple produced by the material. The shear rate q and viscosity are found from the following:

$$q = 2\pi \frac{\Omega}{\varepsilon} \tag{7}$$

$$\eta = \frac{3}{2\pi} \frac{C\varepsilon}{R^3 \Omega} \tag{8}$$

C = measured couple, Ω = angular rotation in cycles/sec
R = radius of cone, ε = angle between cone and plate

D. Flow birefringence

Measurements were made in the 1,2 plane. The quantities measured being the difference Δn in principal refractive indices, the orientation χ of the refractive index ellipsoid to the flow lines and the applied shear rate (q). To obtain the normal stress difference $p_{11} - p_{22}$ from flow birefringence measurements, use must be made of the stress-optical law. For shear flow the latter can be expressed by the relation:

$$p_{12} = \frac{\Delta n \sin 2\chi}{2C} \tag{9}$$

$$p_{11} - p_{12} = \frac{\Delta n \cos 2\chi}{C} \tag{10}$$

335

where
$$C = \frac{2\pi}{45\,kT} \frac{(\bar{n} + 2)^2}{\bar{n}} (a_1 - a_2)$$

according to the theory of rubberlike elasticity[5].

To obtain $(p_{11} - p_{22})$ from relation (10) it is necessary to ensure the validity of the law. This can be done by checking the proportionality of the Shear stress p_{12} to $\Delta n \sin 2\chi$.

E. Dynamic viscosity

A sinusoidal simple shear stress of small amplitude is applied to the material. The amplitude and phase lag of the consequent sinusoidal strain deformation is measured as a function of the applied frequency. The real $G'(\omega)$ and imaginary $G''(\omega)$ components of the complex shear modulus G^* were then derived as functions of the frequency ω in radians per second. It is a requisite that change of the strain amplitude does not affect the values of G' or G''.

F. Stress relaxation

Measured is the relaxation of the shear stress on cessation of steady shearing whilst the material is constrained.

5. THE RESULTS

Viscosities from steady flow measurements

Laboratories I and II had made their measurements for the most part at temperatures of 150°, 160°, 180° and 200°C, it was felt, therefore, convenient to reduce by interpolation the results of III and IV to these temperatures. Extrapolation to the higher temperatures was not considered justified in the odd case where only measurements at lower temperatures were reported.

Figures 1 a–f compare some of the elemental results found by the participants, i.e. the results which as far as possible were directly experimentally obtained and minimally processed. The shear rate range in these figures $10°–10^3 \sec^{-1}$ was particularly chosen so as to cover the region where the cone-and-plate results (II) overlap the capillary and slit results (I, III and IV). It is seen that agreement between the different laboratories is but moderate. However, in view of the fact that here a comparison is made between a mixture of real and apparent shear rates and stresses the differences are not surprising.

In *Figures 2 a–f*, an attempt has been made to remedy this by including Rabonowitch corrections into the results after the manner indicated by Equations (1) and (4).

The polystyrenes

There is evidence that narrow molecular weight distribution materials have small entrance corrections[6, 7] and in particular those for S 111 appear to be negligible[8]. B 8 does not seem to be a polystyrene of particularly broad molecular weight distribution. The neglect of entrance corrections would therefore appear to be justified in these cases.

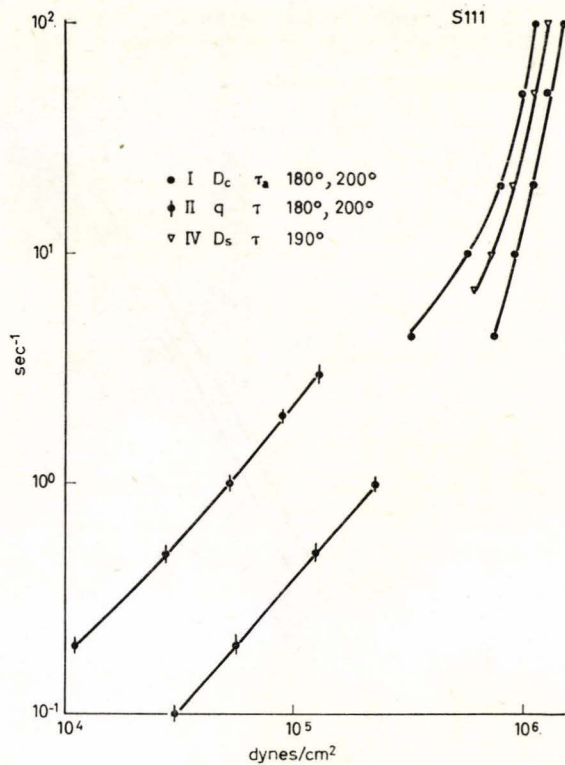With respect to S 111, the measurements obtained by the participants

Figure 1 a. Results obtained for S 111 without application of Rabinowitch corrections.
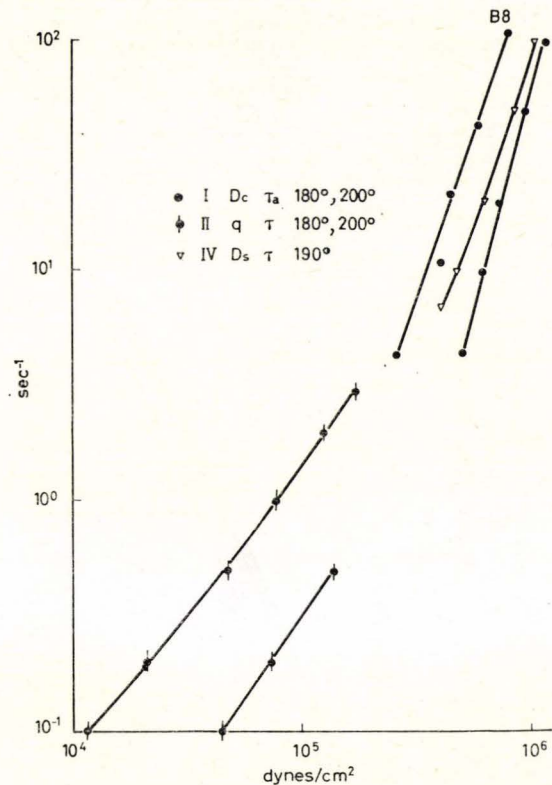
Figure 1 b. Results obtained for B 8 without application of Rabinowitch corrections.
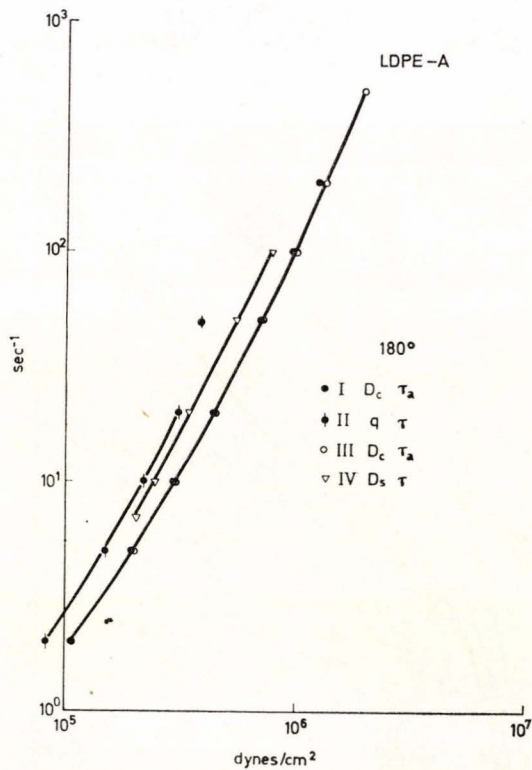
Figure 1 c. Results obtained for LDPE-A without application of Rabinowitch corrections.
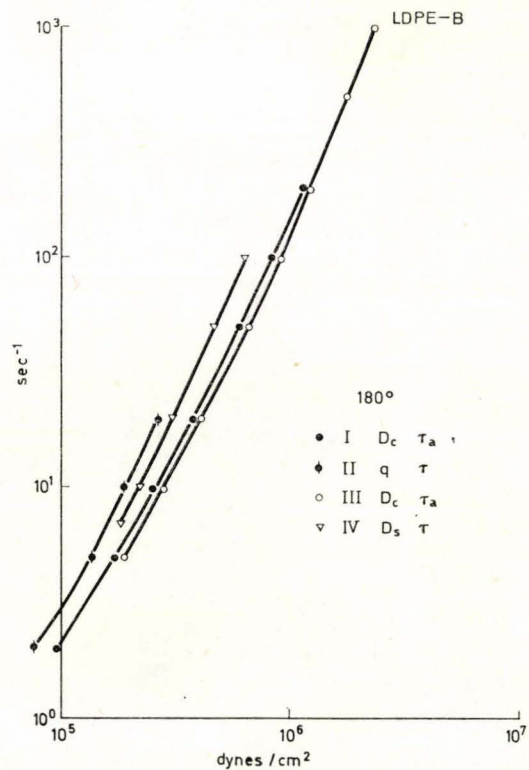
Figure 1 d. Results obtained for LDPE-B without application of Rabinowitch corrections.
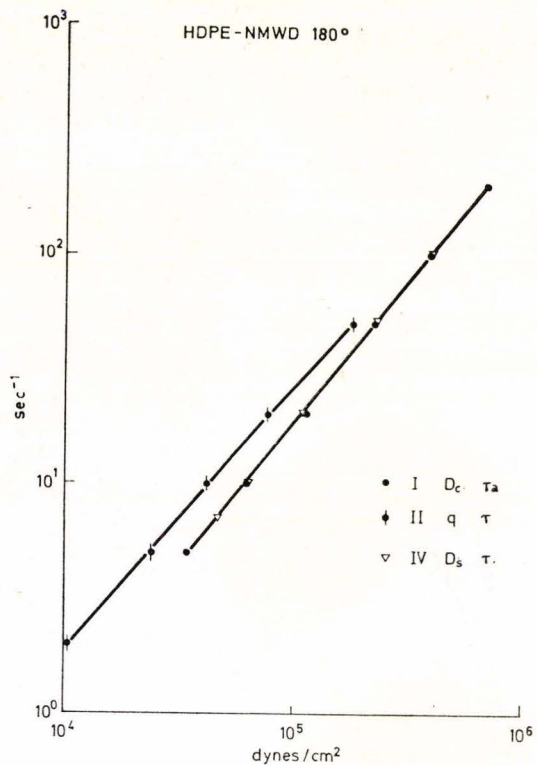
Figure 1 e. Results obtained for HDPE-NMWD without application of Rabinowitch corrections.
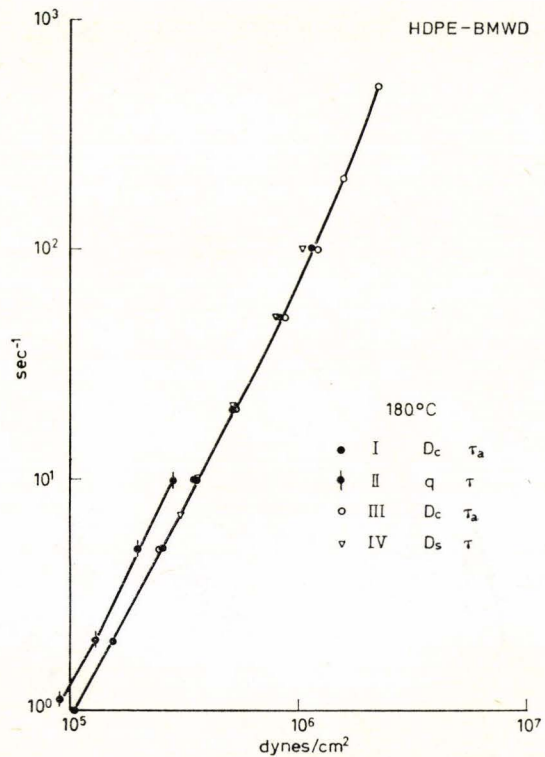

Figure 1 f. Results obtained for HDPE-BMWD without application of Rabinowitch corrections.
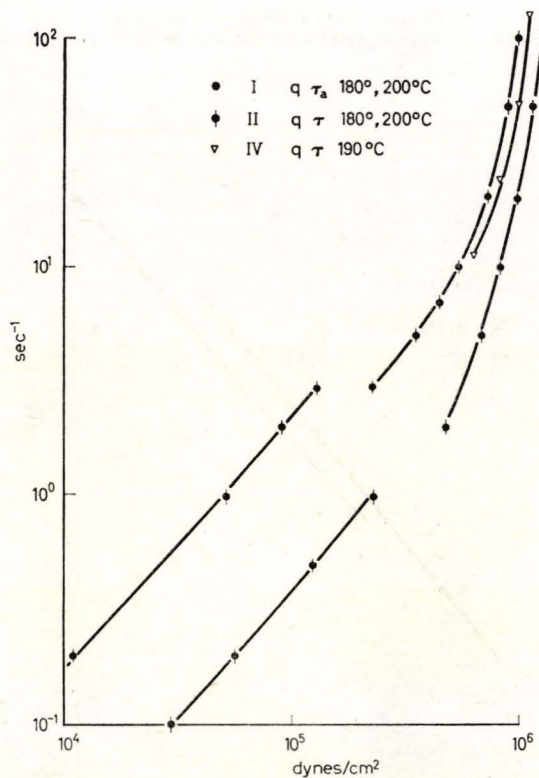
Figure 2 a. Results obtained for S 111 with Rabinowitch
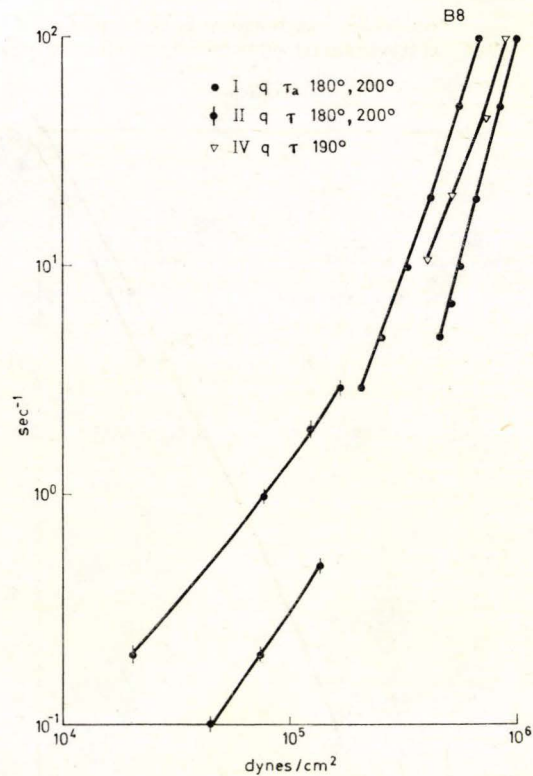corrections.

Figure 2 b. Results obtained for B 8 with Rabinowitch
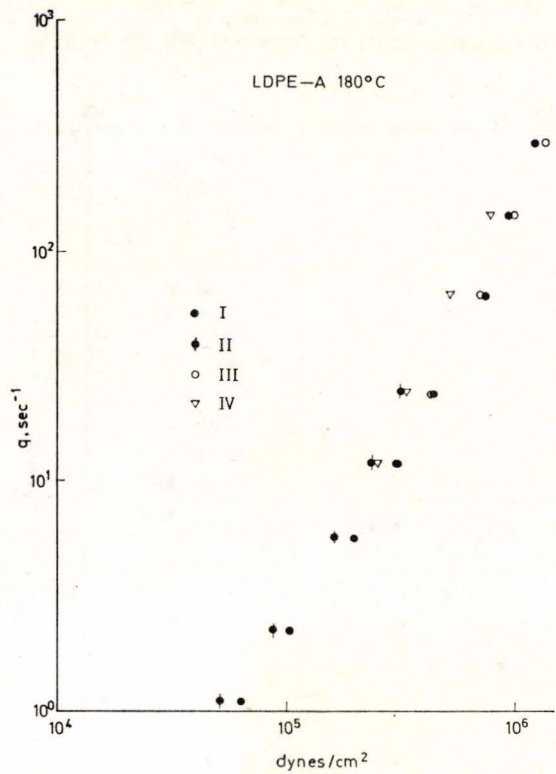corrections.

Figure 2 c. Results obtained for LDPE-A with Rabinowitch corrections.
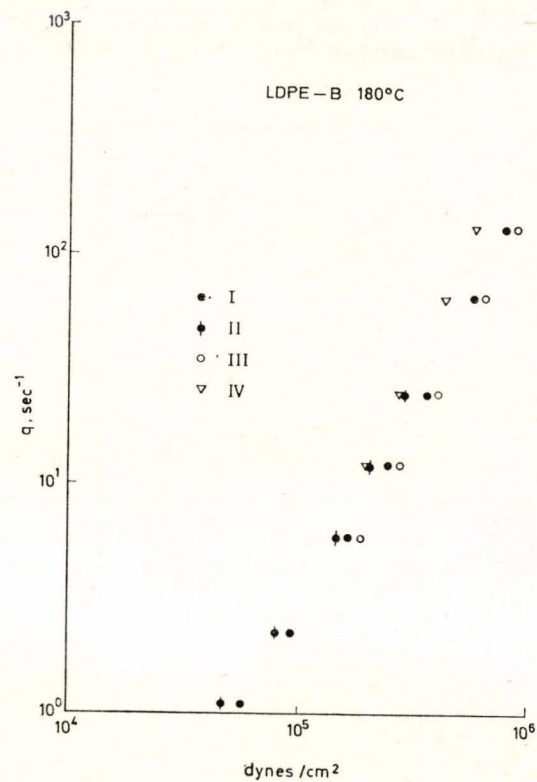

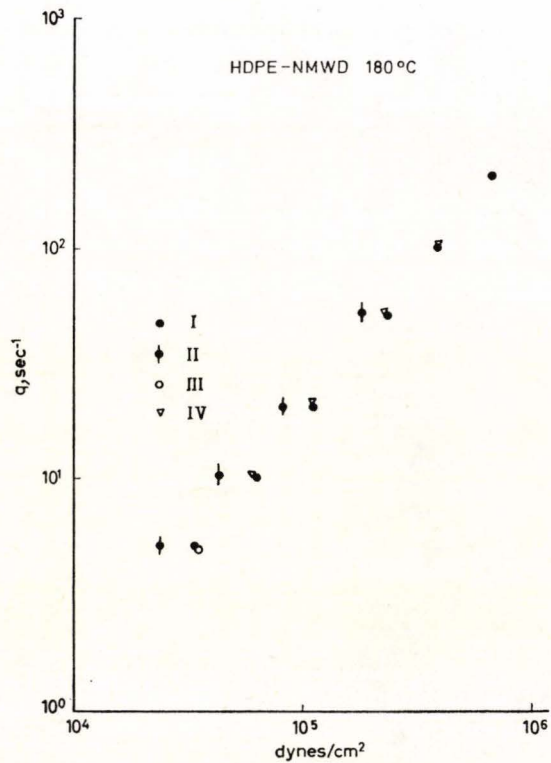*Figure 2 d.* Results obtained for LDPE-B with Rabinowitch corrections.

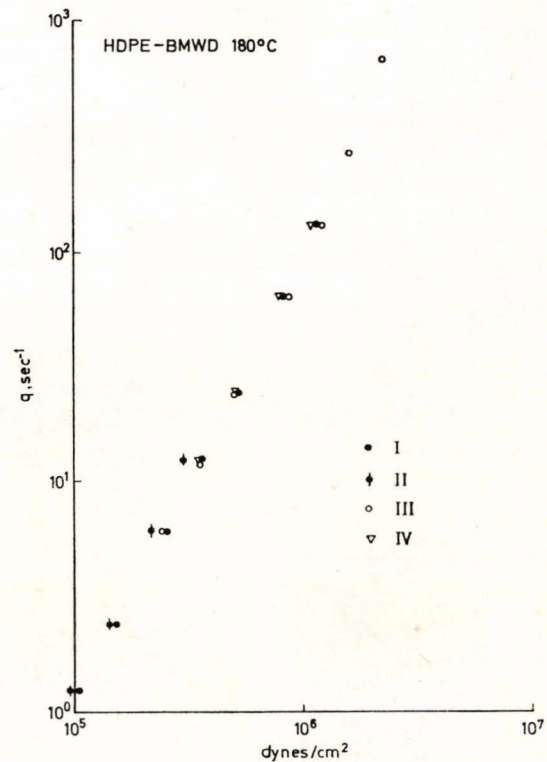*Figure 2 e*. Results obtained for HDPE-NMWD with Rabinowitch corrections.

Figure 2 f. Results obtained for HDPE-BMWD with Rabinowitch corrections.

were not in overlapping shear rate ranges. At 200°C (*Figure 2 a*) I appeared to have nearly reached the Newtonian region of viscosities. In this region one also expects the curves of I and II to line up. They do not. The slit measurements seem to be consistent with the capillary measurements of I.

With respect to B 8, again the cone-and-plate and capillary results were not obtained in the overlapping shear rate region. However, they do appear in this case to be more consistent with one another.

Low density polyethylenes

Figures 2 c and *2 d* show some results obtained when Rabinowitch factors have been applied. The agreement between the laboratories has not been markedly improved by the introduction of the Rabinowitch factors. Nevertheless, all participants agree that the viscosities of the samples A and B scarcely differ from one another at all temperatures and shear rates.

High density polyethylenes

Figures 2 e–f show results obtained with the application of Rabinowitch corrections. Agreement is improved, but it only becomes good in the case of HDPE-BMWD.

These samples show markedly different viscosities and viscosity behaviour. At low shear rates the difference amounts to a factor of about 80, at the highest shear rates the difference has been reduced to a factor less than 2. This behaviour is in contrast to that of the low density polyethylenes.

Comparison of η_0 (for polyethylenes) with results from the literature

$\eta_0 M_w$ relations have been obtained for high density polyethylenes by several authors. *Figure 3* shows η_0, M_w relations for high density polyethylenes as proposed by Tung[9], Ferguson *et al.*[10], Schreiber *et al.*[11] and Peticolas and Watkins[12]. All equations are reduced to 150°C. The results of Tung coincided with those given in references 11 and 12 when he used M_w-values directly from light scattering measurements and not from [η] and [η], M_w relations. Extrapolated Newtonian viscosities obtained in this investigation are also given. It can be seen that those on HDPE-NMWD and HDPE-BMWD are in accordance with the proposals from literature. Theoretical[13] and experimental evidence[14, 15] indicating that the Newtonian viscosity of broad molecular weight distribution materials should depend upon molecular weight averages higher than M_w, were not substantiated even for HDPE-BMWD. The accepted origin of the deviation of low density polyethylenes from such simple η_0, M_w relation is long chain branching. In this connection the closeness of LDPE-A to the published results for high density polyethylenes might indicate that its branches are mainly short ones. It is, however, probably only safe to infer that the branched structure of LDPE-B is different to that of LDPE-A, as the influence of branching upon the Newtonian viscosity is still a matter of some controversy.

Activation energies from steady flow measurements

The apparent energy of activation E_a of steady shear flow has been obtained from the following equation:

$$E_a = 2 \cdot 3R \, \frac{\mathrm{d} \log \eta}{\mathrm{d}(1/T)} \tag{11}$$

Figures 4 a–c show the results obtained. For laboratories I and III the results are of E_a obtained at constant apparent shear stress τ_a. For II and IV the results were obtained at constant shear stress τ.

Polystyrenes

The results obtained by laboratories I and II are given in *Figure 4 a*. The activation energies were obtained from the temperature interval 180–200 °C directly from the measurements made at these temperatures. It appears that both materials have essentially the same apparent activation energies of flow. The values obtained seem to lie somewhat lower than 36 kcal/mole, which the formula of Cox and Ballman predicts at 190 °C[16].

$$\log \eta_0 = 3 \cdot 4 \log M + \frac{900 \cdot 2}{T - 306 \cdot 4} - 18 \cdot 38 \tag{12}$$

Rudd found an apparent energy of activation at 227 °C, which is also lower than would be predicted by the above formula[17].

Low density polyethylenes

The results are given in graphical form in *Figure 4 b*. These results were obtained from smoothed curves of the temperature dependence of viscosity. Within experimental error it appeared that E_a was substantially independent of temperature.

With increasing shear stress there appears to be some decrease in E_a. This effect has been noted by other authors for low density polyethylenes[18–20]. It is thought that the effect is involved with chain branching, however, it remains obscure.

High density polyethylenes

The results given in *Figure 4 c* were obtained in a similar way to the low density polyethylenes. The scatter is rather large. It appears that E_a does not significantly change with shear stress for either of the polymers and the values obtained: 7 kcal/mole for HDPE-NMWD and 6 kcal/mole for HDPE-BMWD are very close to published values[10, 18, 21–24] for linear polyethylenes.

In this connection it is interesting to note that Mills, Moore and Pugh[25] reported a decrease in apparent activation energy with increased broadness of molecular weight distribution for some polyethylene blends. Also some old results of Fox and Flory[26] are of interest—they showed (for polystyrene) that when M_n was less than the critical molecular weight for entanglements (about 25 000 for polystyrene), the apparent energy of activation decreased.
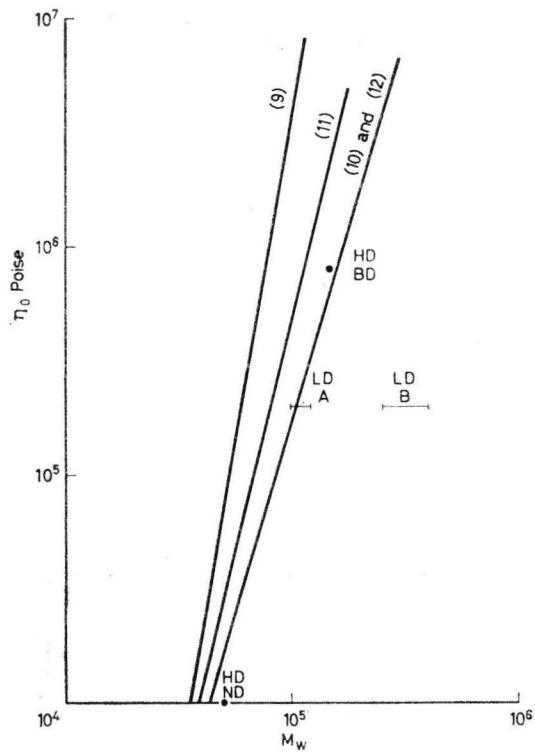
Figure 3. Newtonian viscosities at 150°C for the polyethylenes compared with data from literature.

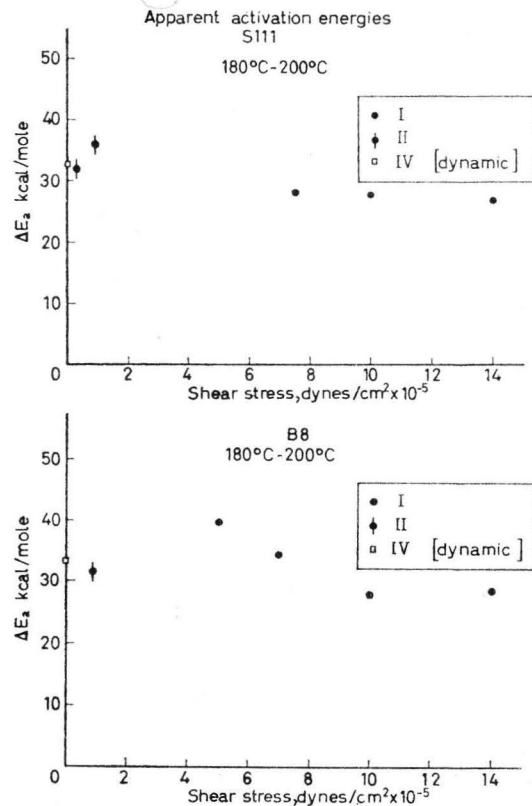Figure 4 a. Apparent energies of activation for polystyrenes as function of the shear stress from steady shear flow measurements.
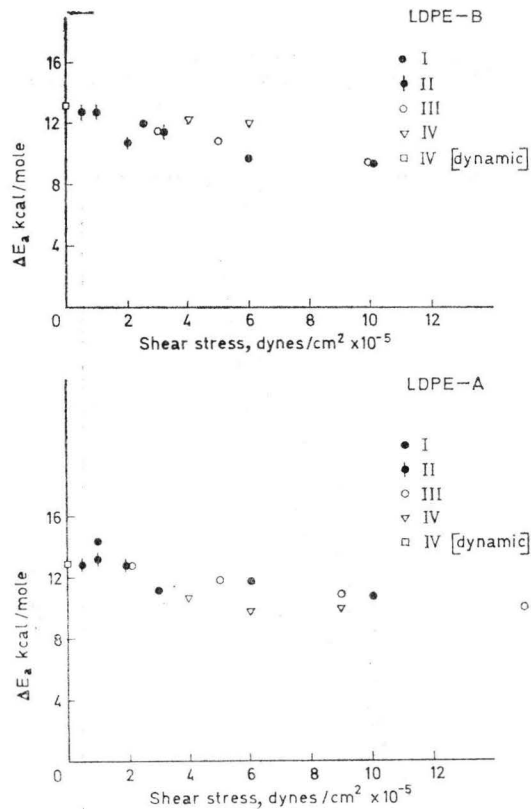
Figure 4 b. Apparent energies of activation for low density polyethylenes as function of the shear stress from steady shear flow measurements.
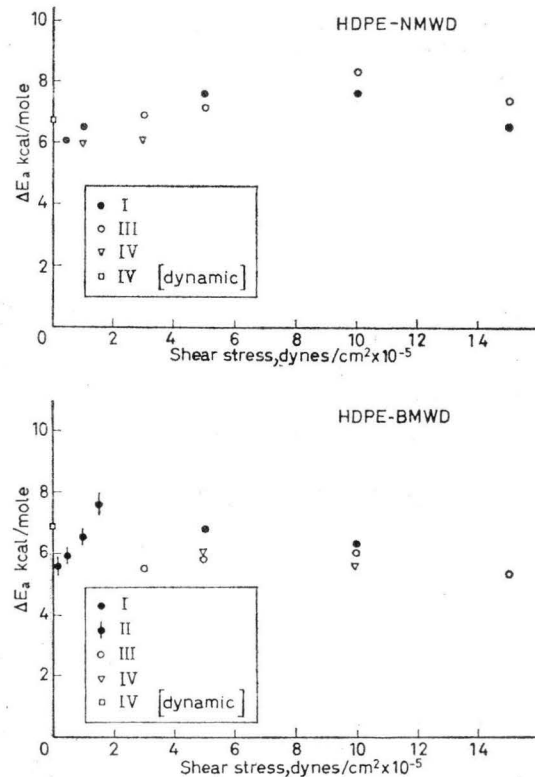

Figure 4 c. Apparent energies of activation for high density polyethylenes as function of the shear stress from steady shear flow measurements.

Dynamic measurements

Figures 6 a–d contain the reduced moduli G'_r, G''_r as functions of frequency. Regularly throughout the measurements checks were made by doubling the amplitude of the oscillation to ensure that the deformation was in the linear region, i.e. the G's remained independent of the amplitude. Measurements at different temperatures were reduced to 190°C by the method of reduced variables. As in well-known, the modulus $G^*_1 (\omega)$ at temperature (T_1) and frequency (ω) is related to the modulus G^*_2 at temperature T_2 by the relation:

$$\frac{G^*_1 (\omega)}{\rho_1 T_1} = \frac{G^*_2 (a_T\omega)}{\rho_2 T_2} \; ; G_r = \frac{G}{\rho T} \tag{13}$$

where ρ_1, ρ_2 are the densities at T_1 and T_2, and a_T is a shift factor with respect to temperature T_1.

The following relations were used by IV for ρT.

$$\rho T = 400 + 0\cdot82 \, (T - 125) \text{ for polystyrene}$$
$$\rho T = 330 + 0\cdot55 \, (T - 150) \text{ for polyethylene}$$

where $T = T°C$.

According to IV, this method of reducing all measurements to one temperature was satisfactory. Frequency reduction factors a_T, obtained from G'' and G', usually agreed to within 5 per cent. The experimentally found shift factors are given in *Figures 5a–b*. An apparent energy of activation H_a can be obtained.

$$H_a = 2\cdot3 \frac{R d(\log a_T)}{d(1/T)} \tag{14}$$

Owing to the introduction of ρT factors H is expected to be somewhat larger than the apparent activation energy from steady flow. The difference is small at 190°C amounting to about 0·7 kcal/mole for polyethylenes and 0·8 kcal/mole for polystyrenes. *Figures 4a–c* contain apparent activation energies from the dynamic measurements after correction for this effect. It is seen that good agreement is found with steady flow apparent activation energies.

Polystyrenes

Apart from the low frequency end of the scale, B 8 and S 111 do not greatly differ in their behaviour. S 111 has a clear maximum and minimum in the G''_r curve, which has been attributed to physical crosslinks. This feature is not present in the same curve for B 8. According to a theory of Marvin[27a], it is possible to calculate the molecular weight between successive entanglements (M_c) when a maximum occurs in G''. Such calculation gave $M_c = 30\,000$ from S 111.

Low density polyethylenes

Over the complete frequency range there is scarcely any difference between the two low density polyethylenes.
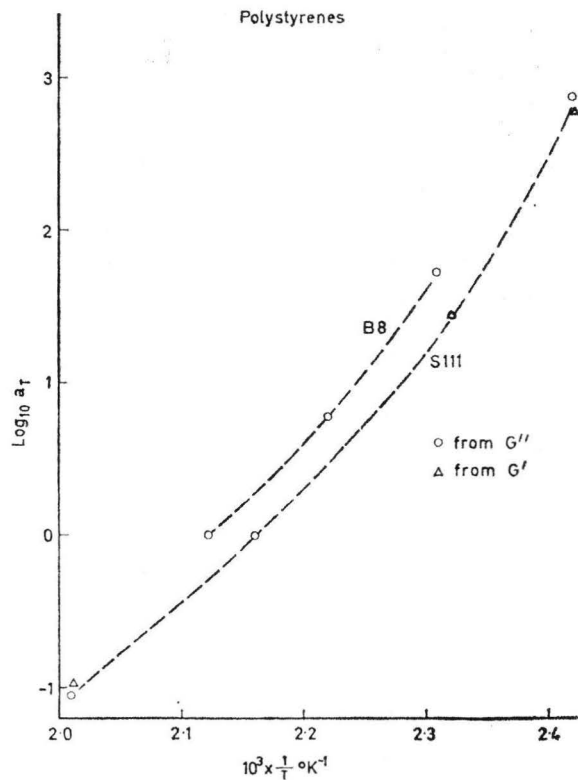
347

Figure 5 a. Shift factor a_T for the polystyrenes as used by IV in the dynamic viscosity measurements.
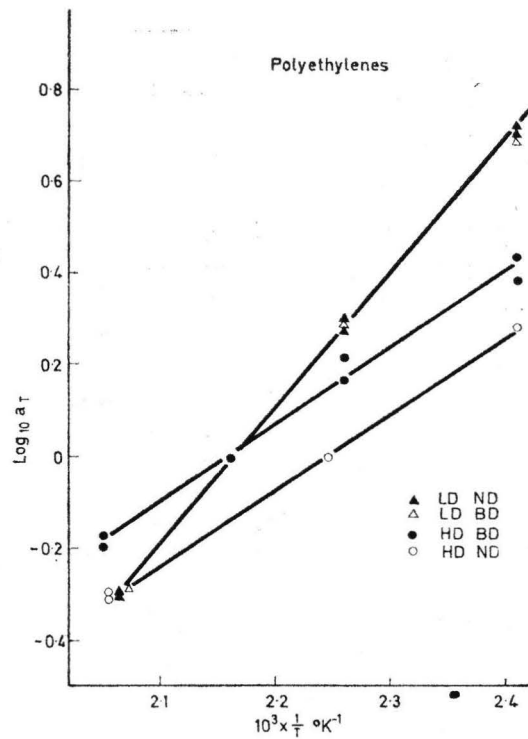
Figure 5 b. Shift factor a_T for the polyethylenes as used by IV in the dynamic viscosity measurements.

Figure 6. (*a*) The reduced modulus $G'/\rho T$ as function of frequency for the polystyrenes. (*b*) The reduced modulus $G''/\rho T$ as function of frequency for the polystyrenes. (*c*) The reduced modulus $G'/\rho T$ as function of frequency for the polyethylenes. (*d*) The reduced modulus $G''/\rho T$ as function of frequency for the polyethylenes.

High density polyethylenes

There are very noticeable differences between the two high density polymers, especially at the low frequency end. At the high frequency end the differences became less noticeable.
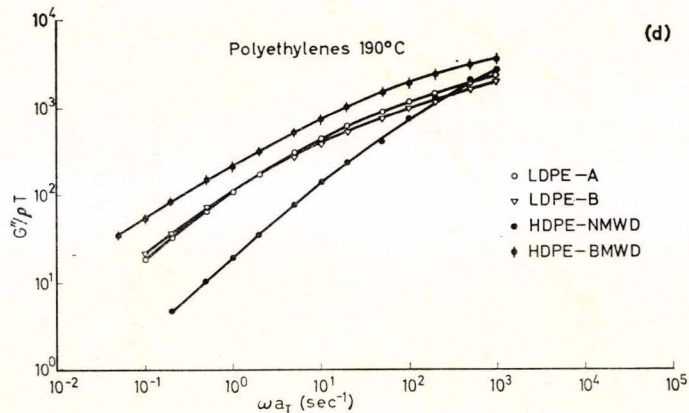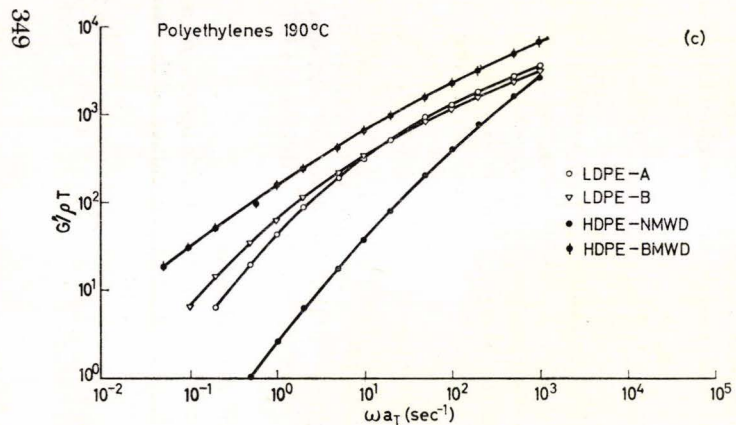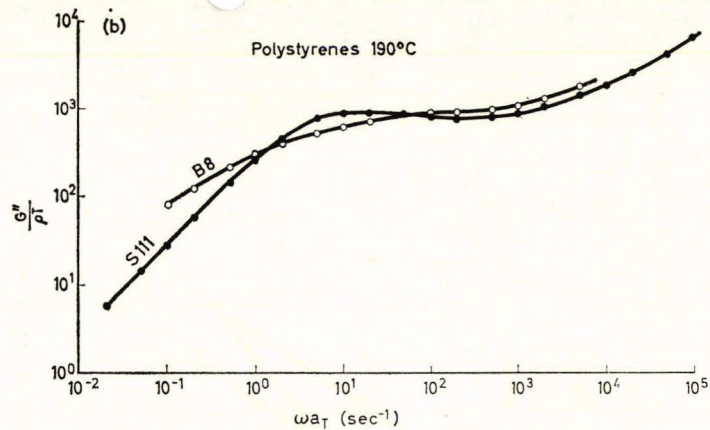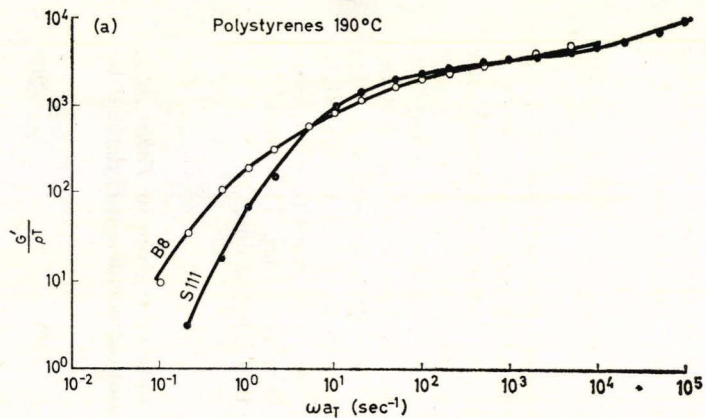
Spectra

For each of the materials the spectrum of relaxation times $H(\tau)$ was calculated by the approximation method of Ninomiya and Ferry[28]. The formulae inter-relating the dynamic moduli with $H(\tau)$ are:

$$G'(\omega) = \int_{-\infty}^{\infty} \frac{H(\tau)\omega^2\tau^2}{1 + \omega^2\tau^2}\, d\,(\ln \tau) \tag{15}$$

$$G''(\omega) = \int_{-\infty}^{\infty} \frac{H(\tau)\omega\tau}{1 + \omega\tau^2}\, d\,(\ln \tau) \tag{16}$$

Figures 7a–c show the reduced spectra $H_r = H/\rho T$ at a temperature of 190°C. The spectra $H(\tau)$ contain in principle no further information than the moduli—the relative behaviour of the broad and narrow molecular weight distribution materials remains the same.

Comparison between steady flow and dynamic viscosities

There have been various suggestions as to how one should compare steady flow viscosities with dynamic viscosities. In the limit of low shear rates and frequencies a simple relation should exist between the two.

$$\eta_s(0) = \lim_{q \to 0} \frac{p_{12}}{q} = \eta'(0) = \lim_{\omega \to 0} \frac{G''}{\omega} \tag{19}$$

Despite the apparently experimental fact for bulk polymers that in steady shear flow at finite shear rates some structural change occurs[8, 29, 30], it has been suggested that one-to-one relations exist between the steady state visocisity at finite q and the dynamic viscosity η at some finite ω[31, 32].

Experimentally the correspondence $\eta_s(q) = |\pi^*(\omega)|$ has been noted[33, 34]. *Figures 8a–f* show comparison between the steady flow viscosities and the dynamic viscosities η' and $|\eta^*(\omega)|$. It is clearly seen that, indeed, in the high shear rate range, $|\eta^*(\omega)|$ is a good approximation to $\eta(q)$ for all the materials. Serious differences are noted, however, at low shear rates in some cases between the limiting dynamic and steady shear viscosities. The reason for this is mysterious and it is difficult to believe that it is genuine.

Flow birefringence

Data from the flow birefringence measurements are given in *Tables 3a–c*. In *Figures 10* are given values of the stress-optical coefficient C defined by the relationship:

$$C = \frac{\Delta n \sin 2\chi}{2p_{12}} \tag{20}$$
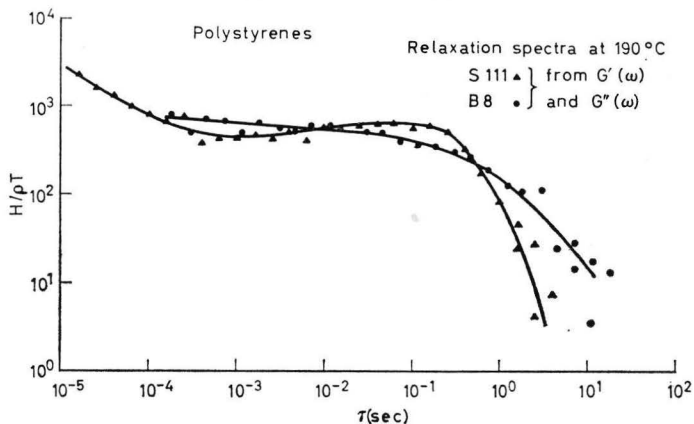
Figure 7 a. Relaxation spectra for the polystyrenes as obtained from the dynamic moduli G' and G'' by the method of Ninomiya and Ferry.
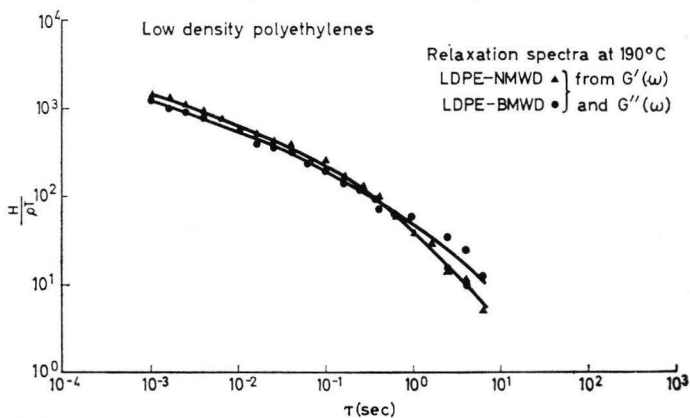
Figure 7 b. Relaxation spectra for the low density polyethylenes as obtained from the dynamic moduli G' and G'' by the method of Ninomiya and Ferry.
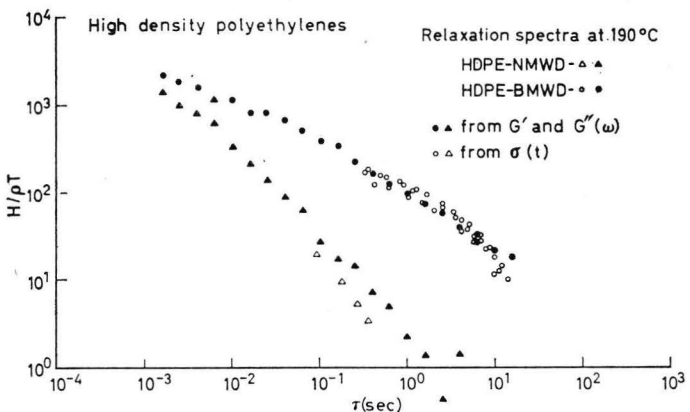
Figure 7 c. Relaxation spectra for the high density polyethylenes as obtained from the dynamic moduli G' and G'' by the method of Ninomiya and Ferry. Also shown in this graph are the relaxation spectra obtained by the method of Ferry and Williams from stress-relaxation measurements.

351
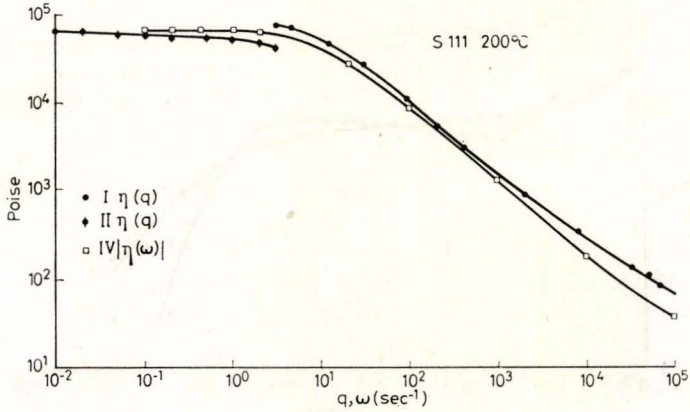
Figure 8 a. The course of the steady shear flow viscosity for S 111 at 200°C as compared with the dynamic viscosity.
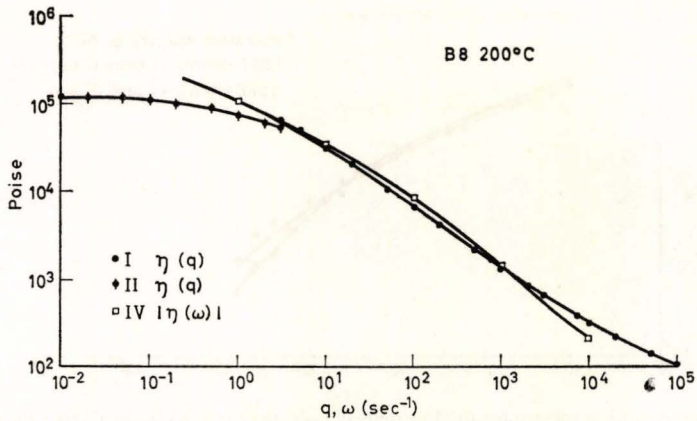
Figure 8 b. The course of the steady shear flow viscosity for B 8 at 200°C as compared with the dynamic viscosity.
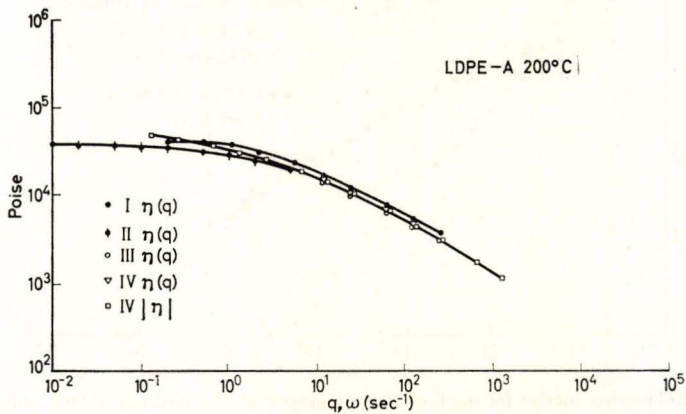
Figure 8 c. The course of the steady shear flow viscosity for LDPE-A at 200°C as compared with the dynamic viscosity.

352
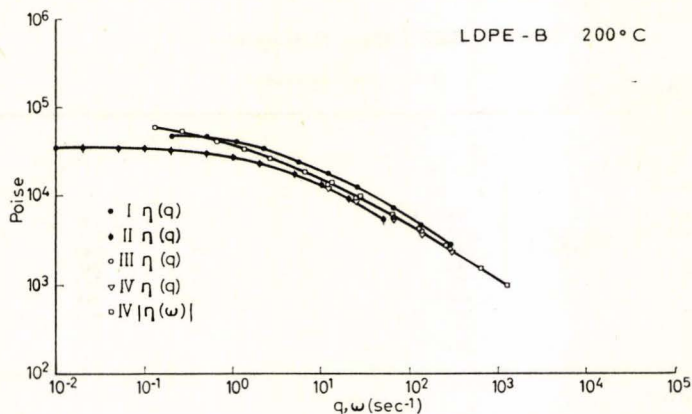
Figure 8 d. The course of the steady shear flow viscosity for LDPE-B at 200°C as compared with the dynamic viscosity.

Figure 8 e. The course of the steady shear flow viscosity for HDPE-NMWD at 150°C as compared with the dynamic viscosity.

Figure 8 f. The course of the steady shear flow viscosity for HDPE-BMWD at 200°C as compared with the dynamic viscosity.

353

Table 3. Flow birefringence

(a) High density polyethylenes

NMWD

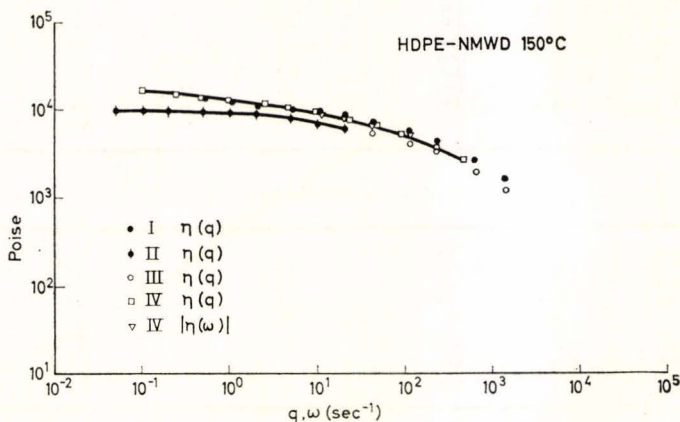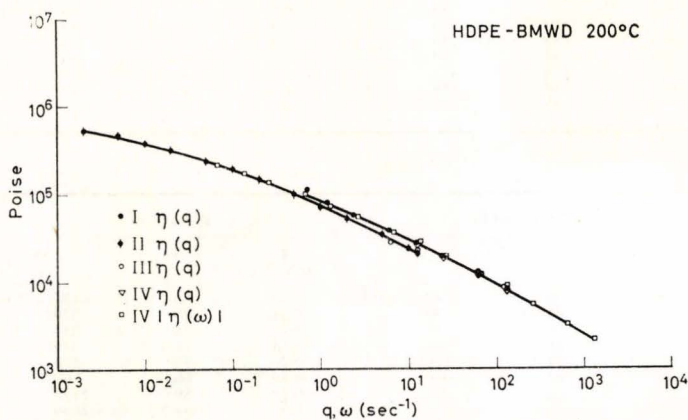|	150°C			190°C	
q (sec^{-1})	$2\chi°$	Δn	q (sec^{-1})	$2\chi°$	Δn
0·3	—	13×10^{-7}	2	80	50×10^{-7}
0·5	86·5	23	6	77	122
0·7	85	33	10	75	188
1	83·5	46	15	73	265
2	80	88	20	71·5	330
3	78	128	30	69·5	464
5	75	200	40	68	580
7	73	270	70	66	900
10	71·5	365			

BMWD

	150°C			190°C	
0·02	64·5	55×10^{-7}	0·02	62	29×10^{-7}
0·03	60	75	0·03	59	39
0·05	57	108	0·05	56·5	56
0·07	55·5	138	0·07	55	70
0·1	54	175	0·1	53·5	90
0·2	53·5	280	0·2	53	145
0·3	51·5	360	0·3	53	190
0·5	50	490	0·5	51·5	250
0·7	49	590	0·7	51	320
1·0	48·5	720	1·0	50	410
2·0	—	—	2·0	49·5	630

(b) Low density polyethylenes

A

0·02	—	18×10^{-7}	0·1	82	21×10^{-7}
0·03	81	26	0·2	78	41·5
0·05	76·5	44	0·3	74	60
0·07	73·5	60	0·5	68	93
0·1	70	85	0·7	65	131
0·2	64	160	1	61	183
0·3	60	225	2	55	349
0·5	55	340			
0·7	52	450			

B

0·05	—	40×10^{-7}	0·1	78	23×10^{-7}
0·07	—	55	0·2	72	46
0·1	70	75	0·3	68	69
0·2	60	140	0·5	61	103
0·3	54	200	0·7	56·5	138
0·5	48	312	1	52	192
0·7	46	410	2	46	330
1	(43·5)	(515)	3	44·5	442

(c) Polystyrenes

	S 111 at 196°C			B 8 at 190°C	
q (sec^{-1})	$2\chi°$	Δn	q (sec^{-1})	$2\chi°$	Δn
0·05	89·5	-42×10^{-7}	0·06	82	-155×10^{-7}
0·07	89·25	-58	0·08	80	-210
0·10	89	-85	0·10	78	-240
0·15	88	-128	0·15	74·5	-340
0·20	87·5	-170	0·20	72	-425
0·50	84	-440	0·40	66	-760
0·70	82	-620	0·70	59	-1155
1·0	79·5	-870	1·0	54·5	-1560
1·5	75·5	-1250	1·2	51	-1625
2·0	71·5	-1650			

The subscripts II and IV refer to the means of estimating p_{12} the shear stress. The apparatus only enables one to measure the dependency of the birefringence and extinction angle on the applied shear rate. C_{II} was obtained by estimation of p_{12} from the cone-and-plate measurements of II and C_{IV} was obtained by equating p_{12} with $|G^*|$ from the dynamic viscosity measurements of IV (with $q = \omega$).

The differences noted in the previous section between $\eta(q)$ and $|\eta(\omega)|$ are reflected by differences in C from the two methods. According to Saunders[35] the stress-optical coefficient of crosslinked linear polyethylene should decrease with increasing temperature from about $2 \cdot 2 \times 10^{-10}$ cm²/ dyne at 150°C to $1 \cdot 7$–$1 \cdot 8 \times 10^{-10}$ cm²/dyne at 190°C. The experimental data can be said to be consistent with this.

One expects branched materials to have somewhat different stress-optical coefficients to linear ones. This effect is probably small for the low density polyethylenes as the frequency of branching is low ($1 \cdot 2$ to $1 \cdot 5$ CH_3-groups per 100 CH_2-groups). This is borne out by the results which indicate that the stress-optical coefficient of the LDPE's is approximately the same as that of the HDPE's.

There are no satisfactory stress-optical measurements reported on polystyrene at temperatures well in excess of the glass temperature. The C-values found here are larger than would be expected from the room temperature (solution) values when one factors by the expected kT terms according to the simple theory of rubber-like elasticity. This could qualitatively be taken to indicate that the end-to-end distance of polystyrene in bulk will increase with increase of temperature. The probable presence, however, of a transition at about 80°C[36] should also be taken into account.

Current molecular theories for the behaviour of bulk molten polymers have largely been direct transplantations of dilute solution theories. A direct comparison between dilute solutions and bulk measurements could provide some indication of the validity of the approach. One of the simplest ways to do this is to eliminate the friction factor occurring in the molecular theories by plotting the reduced shear stress $(p_{12})_r$ contribution due to the macromolecules against the reduced normal stress difference: $\frac{1}{2}(p_{11} - p_{22})_r$. These quantities being defined:

$$(p_{12})_r = (\eta - \eta_0)q \frac{M_w}{cRT} \qquad \text{(solution)}$$

$$= \eta(q)q \frac{M_w}{\rho RT} \qquad \text{(melts)} \tag{21}$$

$$\frac{1}{2}(p_{11} - p_{22})_r = \frac{1}{2}(p_{11} - p_{22}) \frac{M_w}{cRT} \qquad \text{(solutions and melts)}$$

The concentration c is expressed in g/ml so as to correspond with ρ when dealing with the bulk material.

According to the Rouse theory[37], the relationship between these quantities should, at sufficiently low shear rates be (cf. ref. 38):

$$\frac{1}{2}[p_{11} - p_{22}]_r = \frac{2}{5} \left(\frac{M_z}{M_w}\right)^2 \left(\frac{M_{z+1}}{M_z}\right) [p_{12}]^2_r \tag{22}$$

The normal stress difference can be found from flow birefringence measurements with the help of the stress-optical law and the stress-optical coefficient (cf. Section 4 D).

According to Equation (22), the quantity

$$\lim_{q \to 0} \frac{1}{2} \frac{[p_{11} - p_{22}]_r}{[p_{12}]^2_r} = P_w \tag{23}$$

should only be dependent on the shape of the molecular weight distribution of a given linear polymer. P_w expresses a relationship between elastic and viscous terms in steady flow, its connection with the steady state compliance J_e for linear polymers will be noted (cf. ref. 27c).

$$J_e = P_w \frac{M_w}{cRT} \tag{24}$$

The Rouse theory has also been applied to some particular cases of molecules[39] branched in a regular way—for the most general type of branched structure the theory becomes unmanageable and it is only possible to make the qualitative prediction that values of (P_w) should be smaller for branched molecules than for linear molecules with the same molecular weight distribution.

Approximated values of P_w and J_e from the melt measurements are given in *Table 4* together with theoretical values of P_w from the Rouse treatment, with the assumption that the polydispersity factor in Eq. (22) is approximately $(M_z/M_w)^2$ (an underestimate).

Table 4. Approximated values of P_w and J_e from the melt measurements together with theoretical values of P_w from the Rouse treatment

Polymer	M_w/M_n	P_w (Rouse Theory)	P_w (exp.)	J_e (exp.)
S 111	1·04	0·4	0·4–0·45	2·3 cm²/kg
B 8	2·47	—	0·7	5·2
HDPE-NMWD	4–5	10–36	14	13
HDPE-BMWD	~17	20–32	37–90	60–150
LDPE-A	5–8	(6·4)	7	29
LDPE-B	14–17	(52)	4	37

The close agreement of S 111 to the theory of Rouse is evident and the increase of P_w with increased broadness of the molecular weight distribution of the linear polymers is also evident. The low density polymers show a contrary behaviour (branching?).

It should be emphasized that P_w expresses an intrinsic relationship between viscous and elastic terms in steady flow when account has been taken that these depend on the number of molecules present. In view of the doubts that have arisen lately concerning the validity of the molecular theories for bulk polymers[40-42, 45] it might be better to take $\frac{1}{2}[p_{11} - p_{22}]p_{12}$ at a particular shear stress as a measure of the elasticity of the material. It then appears that *all* the broad molecular weight distribution materials are more elastic than their narrow molecular weight distribution counterparts.

At a shear stress just greater than 0.1 kg/cm^2, the ordering from low to high elasticity is:

$$S\ 111 < HDND < B\ 8 < LD\text{-}A < HDBD < LD\text{-}B$$

the last two differing but little from one another. It is noted that the die swell of LD-A was less than that of LD-B. It is also noted that the above ordering is somewhat different from the J_e ordering.
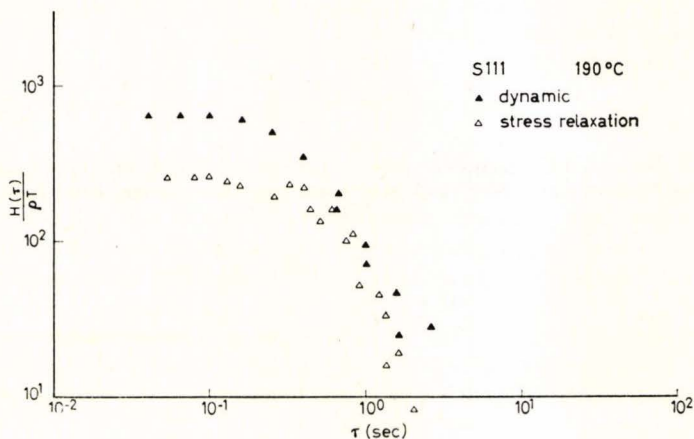

Figure 9 a. The relaxation spectra for S 111 as obtained from the dynamic moduli by the method of Ninomiya and Ferry and from stress relaxation by the method of Ferry and Williams.

Figure 9 b. The relaxation spectra for B 8 as obtained from the dynamic moduli by the method of Ninomiya and Ferry and from stress relaxation by the method of Ferry and Williams.

357

Figure 9 c. The relaxation spectra for LDPE-A as obtained from the dynamic moduli by the method of Ninomiya and Ferry and from stress relaxation by the method of Ferry and Williams.
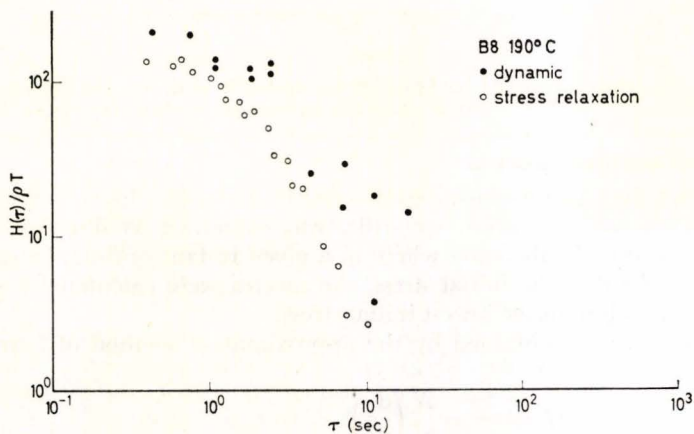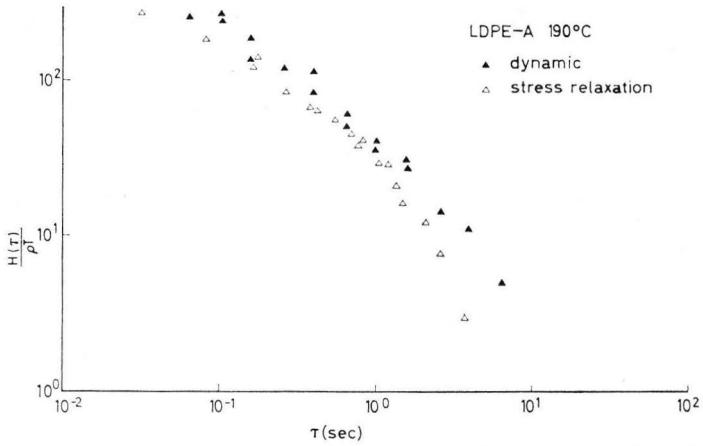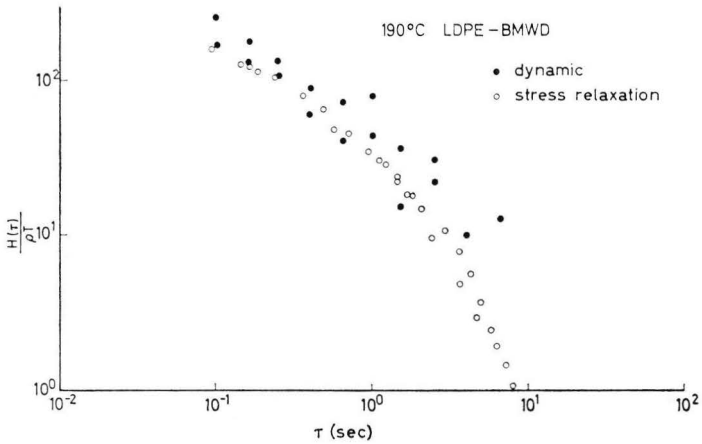

Figure 9 d. The relaxation spectra for LDPE-B as obtained from the dynamic moduli by the method of Ninomiya and Ferry and from stress relaxation by the method of Ferry and Williams.

Stress-relaxation spectra

To check that measurements were carried out in the 'linear' region, the fractional decrease in stress $\sigma(r)/\sigma(0)$, was examined as function of the initial stress $\sigma(0)$. In the cases where at a given instant of time, $[\sigma/\sigma_0]$, was not independent on the initial stress, the spectra were calculated from the data corresponding to the lowest initial stress.

The spectra were obtained by the approximation method of Ferry and Williams[43]:

$$H(\tau) = -\frac{N}{q_0}\left(\frac{d\tau}{dt}\right)_{t=\tau} \tag{24}$$

$$N = [\Gamma(m)]^{-1}; \qquad m = \frac{d \log H(\tau)}{d \log \tau}$$
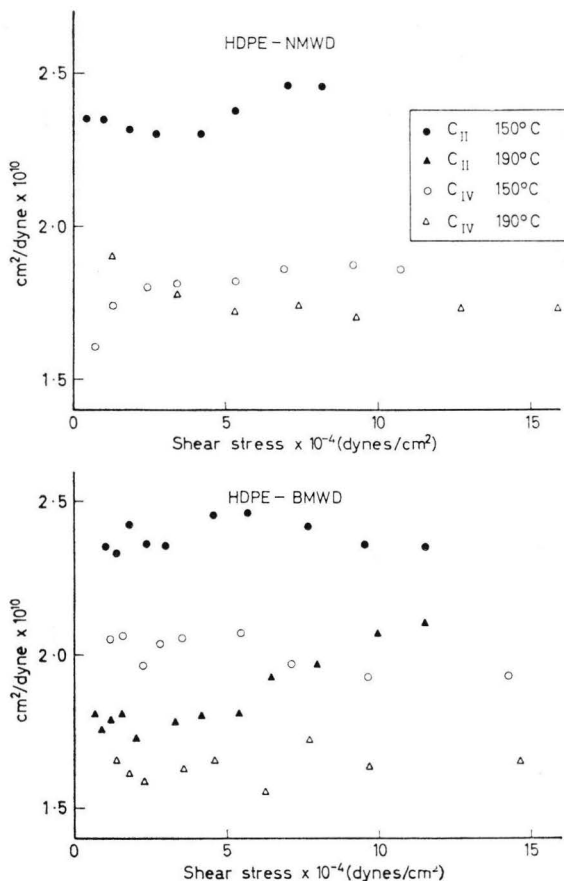
358

Figure 10 a. Stress-optical coefficients obtained from Equation (9), plotted as a function of the shear stress for the high density polyethylenes.

The spectrum H being defined by the relation:

$$\sigma(t) = q \int_0^\infty H(\tau) \exp\left(-t/\tau\right) d\tau \qquad (25)$$

Data at different temperatures have been reduced to one temperature (190 °C) and reproduced in *Figures 7c, 9a–d,* alongside the spectra obtained by IV from dynamic viscosity measurements.

The temperature shift factors were those obtained from steady shear viscosities.

The spectra are given in the reduced form: $H_r = H/\rho T$. The densities used by II were:

$$\rho^{-1} = 0 \cdot 955[1 + 6 \cdot 1 \ (T - 298) \cdot 10^{-4}] \quad \text{for polystyrene}$$

$$\rho^{-1} = 1 \cdot 18 \ [1 + 8 \cdot 6 \ (T - 298) \cdot 10^{-4}] \quad \text{for polyethylene}$$

359

It is seen that, with the possible exception of S 111, the spectra from stress relaxation and from dynamic viscosity measurements are essentially in agreement. Moreover, it is possible that the differences which do exist can be at least partially ascribed to the differences obtained by II and IV between $\eta(0)$ and $\eta'(0)$.

The method of Ferry and Williams presupposes a particular shape of the spectrum of relaxation times, i.e. on a log–log scale it is a linear function. Thus, it is not expected to be a good approximation where more rapid changes of shape occur. This is possibly the reason for the failure of the two methods to agree at short times in the case of S 111. Tobolsky and Murakami[44] suggested that their method would be especially suited in such instances. Their method of obtaining a discrete spectrum allows one in the case of S 111 to obtain an additional check on the Rouse theory.

If the relaxation data are expressed as follows:

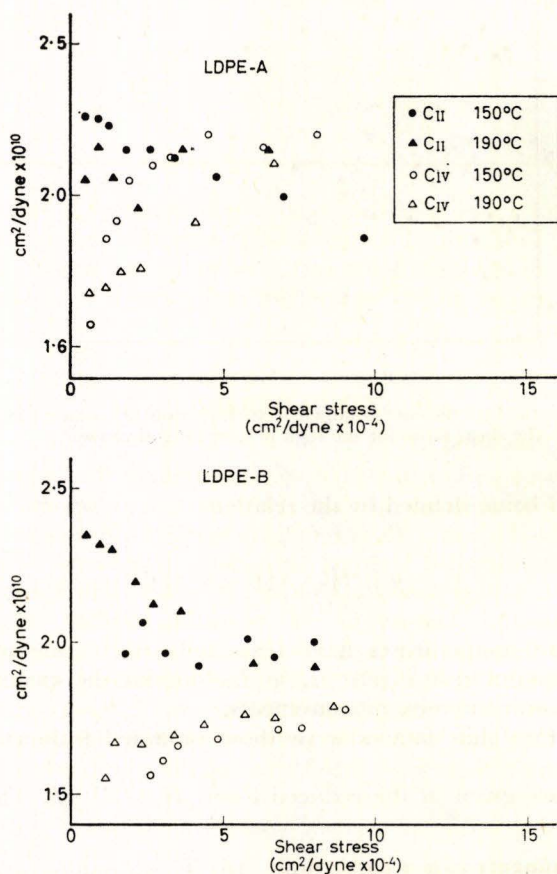$$\sigma(t) = q_0 \, \Sigma \, a_i \tau_i \exp \, (-t/\tau_i)$$

Figure 10 b. Stress-optical coefficients obtained from Equation (9), plotted as a function of the shear stress for the low density polyethylenes.

360

then the Rouse theory applied to melts would give for very narrow molecular weight distributions:

$$a_i = a_j = \frac{\rho RT}{M}$$

$$\tau_{max} = \tau_1 = \frac{6}{\pi^2} \eta_0 \frac{M_w}{\rho RT}$$

$$\tau_p = p^{-2}\tau_1$$

And it follows:

$$\frac{\sigma(t)}{\sigma(0)} = \Sigma\, b_i \exp\, (-t/\tau_i)$$

$$b_1, b_2, \ldots = 0 \cdot 608, 0 \cdot 152, 0 \cdot 068, \ldots \text{ etc.}$$

Table 5. Spectral data of S 111 obtained by the method of Tobolsky and Murakami

Temp. (°C)	τ_1 (sec)	b_1	τ_2 (sec)	b_2	τ_1 (Rouse theory)
150	50	0·72	16	0·23	33
180	1·6	0·83	0·5	0·25	1·3
200	0·28	0·44			0·25

The approximate data given in *Table 5* was obtained by the method of Tobolsky and Murakami. The agreement with the molecular theory is moderate, the τ_1 in two cases being very close to the theoretical. The method is, however, somewhat subjective and not really suited to obtain the short times.

6. CONCLUSIONS

1. Steady flow viscosity

All laboratories agree on the relative behaviour of the broad molecular weight distribution materials to that of the narrow molecular weight distribution materials. However, there remain noticeable differences between the participants in the detailed viscosity behaviour. In general, it can be said that II and IV obtained somewhat lower viscosities than I and III in the region where cone-and-plate measurements overlap capillary measurements. Without further investigation it is not possible to see just why these differences have arisen. Qualitatively part of the difference is certainly due to neglect of entrance corrections on the capillary work, however, considering that I used a capillary with which the entrance corrections should be negligible, it is hard to believe that these are the sole reasons for the discrepancies.

2. Activation energies in steady flow

Good agreement is obtained for apparent energies of activation with published data on polystyrenes and polyethylenes. The found activation

energies are also in agreement with activation energies calculated from the dynamic viscosity shift factors.

3. Dynamic and steady flow viscosities

At higher shear rates, a strong correspondence is found between the absolute value of the dynamic viscosity $|\eta^*(\omega)|$ at frequency ω and the steady flow viscosity $\eta(q)$. This correspondence agrees with earlier findings in the literature. For some of the investigated materials, discrepancies are noted at the lowest shear rates.

4. Spectra

The spectra of relaxation times calculated from stress-relaxation agreed well with those determined from the dynamic moduli $G'(\omega)$ and $G''(\omega)$. The spectra obtained from $G'(\omega)$ and $G''(\omega)$ were the same, indicating close correspondence between elastic and viscous components in the melts, at least in the linear region of viscoelastic behaviour.

5. Flow birefringence

The stress-optical law is, within the uncertainty of the measurements, valid for the flowing melt. Using the extinction angle as a measure of the relationship between the elastic and viscous components, it is found that at a given shear stress, all the broad molecular weight distribution materials were more elastic than their narrow molecular weight distribution counterparts. Almost quantitative support for the Rouse theory as applied to flowing polymer melts is found in the case of one of the polystyrenes. In view, however, of recent evidence in the literature[45] indicating, at least for polystyrene, a possibly more complicated behaviour, no firm conclusion as to this latter point can be made.

6. Stress-relaxation (see Conclusion 4)

It is further noted that semi-quantitative evidence was found here for the application of the theory of Rouse to the melt.

References

[1] E. H. Merz and R. W. Colwell. *ASTM Bull.* **63**, No. 232 (1958).
[2] J. L. S. Wales, J. L. den Otter and H. Janeschitz-Kriegl. *Rheol. Acta* **4**, 146 (1965).
[3] J. L. S. Wales and H. Janeschitz-Kriegl. *J. Polymer Sci.* **A2**, 5, 781 (1967).
[4] J. L. Den Otter. *Rheol. Acta*, to be published.
[5] L. R. G. Treloar. *The Physics of Rubber Elasticity*, Oxford University Press, London, 1958.
[6] H. P. Schreiber and E. B. Bagley. *J. Polymer Sci.* **B1**, 365 (1963).
[7] J. T. Gruver and G. Kraus. *J. Polymer Sci.* **2**, 797 (1964).
[8] R. A. Stratton. *J. Coll. Interface Sci.* **22**, 517 (1966).
[9] L. H. Tung. *J. Polymer Sci.* **46**, 409 (1960).
[10] J. Ferguson, B. Wright and R. N. Haward. *J. Appl. Chem.* **14**, 53 (1964).
[11] H. P. Schreiber, E. B. Bagley and D. C. West. *Polymer, London* **4**, 355 (1963).
[12] W. L. Peticolas and J. M. Watkins. *J. Am. Chem. Soc.* **79**, 5083 (1957).
[13] F. Bueche. *J. Polymer Sci.* **43**, 527 (1960).
[14] K. Sakamoto, K. Kataoka, Y. Fukasawa and H. Funahashi. *Zairyo* **15** (152), 377 (1966).
[15] A. J. De Vries. *Proceedings Fourth Intern. Congress Rheol.* Part 3, 321 (1963) published (1965).
[16] W. P. Cox and R. L. Ballman. *J. Appl. Polymer Sci.* **4**, 121 (1960).
[17] J. F. Rudd. *J. Polymer Sci.* **44**, 459 (1960).

[18] R. Sabia. *J. Appl. Polymer Sci.* **8**, 1651 (1964).
[19] J. Meissner. *Proc. Int. Congr. Rheol.* Brown 1963, Part 3, 437 (1965).
[20] R. A. Mendelson. *S.P.E. Trans.* **5**, 34 (1965).
[21] R. A. Mendelson. *Trans. Soc. Rheol.* **9**: 1, 53 (1965).
[22] E. M. Cernia and C. Mancini. *Polymer Letters* **4**, 71 (1966).
[23] N. Nakajima, G. A. Tirpak and M. Shida. *Polymer Letters* **3**, 1089 (1965).
[24] H. Schott and W. S. Kaghan. *J. Appl. Polymer Sci.* **5**, 175 (1961).
[25] D. R. Mills, G. E. Moore and D. W. Pugh. *S.P.E. Trans.* **1**, 40 (1961).
[26] T. G. Fox and P. J. Flory. *J. Am. Chem. Soc.* **70**, 2384 (1948).
[27] J. D. Ferry, in Viscoelastic Properties of Polymers, Wiley, New York and London, 1961, (a) page 189, (b) page 163, (c) page 171.
[28] K. Ninomiya and J. D. Ferry. *J. Colloid Sci.* **14**, 36 (1959).
[29] G. V. Vinogradov and I. M. Belkin. *J. Polymer Sci.* **3A**, 917 (1965).
[30] S. Krishnamurthy. *Polymer Letters* **5**, 69 (1967).
[31] R. Roscoe. *Brit. J. Appl. Phys.* **15**, 1095 (1964).
[32] Y. H. Pao. *J. Appl. Phys.* **28**, 591 (1957).
[33] W. P. Cox and E. H. Merz. *J. Polymer Sci.* **28**, 619 (1958).
[34] S. Onogi, T. Fujii, H. Kato and S. Ogihara. *J. Phys. Chem.* **68**, 1598 (1964).
[35] D. W. Saunders, D. R. Lighfoot and D. A. Parsons. *J. Polymer Sci.* **A2, 6**, 1183 (1968).
[36] C. Reiss. *J. Chim. Physique Physico Chim.* **63**, 1299 (1966).
[37] J. L. S. Wales and H. Janeschitz-Kriegl. *Rheol. Acta* **7**, 19 (1968).
[38] A. Peterlin. *J. Chem. Phys.* **39**, 224 (1963).
[39] B. H. Zimm and R. W. Kilb. *J. Polymer Sci.* **37**, 19 (1959).
[40] A. V. Tobolsky, J. J. Aklonis and G. Akovali. *J. Chem. Phys.* **42**, 723 (1965).
[41] G. Akovali. *J. Polymer Sci.* **A2, 5**, 875 (1967).
[42] W. F. Busse. *J. Polymer Sci.* **A2, 5**, 1261 (1967).
[43] J. D. Ferry and M. L. Williams. *J. Colloid Sci.* **7**, 347 (1952).
[44] A. V. Tobolsky and K. Murakami. *J. Polymer Sci.* **40**, 443 (1959).
[45] H. J. M. A. Mieras and C. F. H. van Rijn. *Nature* **218**, 865 (1968).